Ultraplankton distribution in surface waters of the Mozambique Channel – flow cytometry and satellite imagery

Mikhail V. Zubkov*, Graham D. Quartly

Southampton Oceanography Centre, European Way, Southampton, SO14 3ZH,United Kingdom

RUNNING HEADING: Ultraplankton distribution in the Mozambique Channel

KEY WORDS: Picoeukaryotic algae, *Synechococcus*, *Prochlorococcus*, cyanobacteria, bacterioplankton, picoplankton, remote sensing, sea surface temperature and colour, chlorophyll

* - corresponding author, address: Southampton Oceanography Centre
European Way
Southampton, SO17 3ZH
United Kingdom
Telephone: +44 (0)23 8059 6335
Fax: +44 (0)23 8059 6247
e-mail: mvz@soc.soton.ac.uk

Abstract

The composition of ultraplankton in near-surface samples collected underway every 1 to 6 h from a ship sailing from Durban to the Seychelles was determined by flow cytometry, using both autofluorescence pigments and fluorescence DNA staining. *Prochlorococcus* (17 to 160 × 10^3 cells ml^{-1}) numerically dominated the ultraphytoplankton, followed by *Synechococcus* (4.5 to 57 × 10^3 cells ml^{-1}) and eukaryotic algae (0.6 to 4.2 × 10^3 cells ml^{-1}). The abundance of heterotrophic bacterioplankton was 0.4 to 1.3 × 10^6 cells ml^{-1}. A strong correlation (r = 0.8-0.97) was observed between SeaWiFS satellite estimates of total chlorophyll concentration and chlorophyll concentration, abundance and biomass of eukarytic algae as well as abundance and biomass of heterotrophic bacteria. This shows the potential for deducing spatial distributions of these two groups for ecosystem modelling using satellite data. Although the correlation between satellite chlorophyll estimates and *Synechococcus* chlorophyll concentration was strong (r=0.83-0.88) the correlation with its abundance and biomass was poor (r < 0.6) due to high variability (factor of 12) in cellular chlorophyll content and to a lesser extent to diurnal cycles. The relationships were similar when either only daytime or all ultraplankton measurements were compared with the satellite data. No relationship was found between satellite data and *Prochloroccocus* chlorophyll concentration, abundance or biomass, even after correction for a pronounced diel cycle, suggesting that the SeaWiFS instrument might not detect *Prochlorococcus* chlorophyll.

Introduction

Monitoring of ocean colour using satellites provides high-resolution data about the spatio-temperal distribution of photosynthetic pigments in the surface waters (Garcon et al. 2001). A valuable addition to space-based studies of primary productivity (Behrenfeld & Falkowski 1997) would be the interpretation of these data in terms of the concentration of certain groups of abundant microorganisms. Considering their concentrations (10^3– 10^6 cells ml^{-1}) and size (0.2 – 5 μm in diameter) ultraplankton (Li 1995) should have the largest effect among organisms on light attenuation and reflection in the surface waters (Morel et al. 1993). In tropical and subtropical oceanic waters ultraphytoplankton account for ~80% of total chlorophyll and phytoplankton biomass as well as for ~70% of total primary production, e.g. (Li & Harrison 2001, Maranon et al. 2001). Eukaryotic algae and cyanobacteria, the two main components of ultraphytoplantkon, contribute equally to ultraphytoplankton biomass (Zubkov et al. 2000b). The carbon standing stock of heterotrophic bacterioplankton, another component of ultraplankton, on average equals that of total phytoplankton (e.g. Li & Harrison 2001). However, despite the apparent ultraplankton domination in tropical to equatorial oceanic waters, according to our knowledge there have been few comparative studies of satellite measurements and in situ concentrations of ultraplanktonic groups.

Using flow cytometry (Olson et al. 1993) ultraplankton can be accurately enumerated and discriminated into three main cytometric groups: namely picoeukaryotic algae; cyanobacteria, *Prochlorococcus* (Chisholm et al. 1988) and *Synechococcus* (Waterbury et al. 1979); and other nonautofluorescent, heterotrophic bacterioplankton. The latter are usually visualised by staining cellular nucleic acids with fluorescence dyes, e.g. (Marie et al. 1997). Another advantage of flow cytometry is the ability to generate large sets of high quality data necessary for studying large-scale distributions of ultraplankton, e.g. (Buck et al. 1996, Li 1995, Li & Harrison 2001, Zubkov et al. 2000a). This ability is particularly useful for validating space-based biological measurements.

In the present study we counted ultraplankton on a meridional transect along the Mozambique Channel with the aim of assessing the possibility of using satellite data for estimating the concentrations of ultraplanktonic groups in the surface waters.

Methods

Sampling site. A total of 65 samples were collected from 23 to 29 August 2001 during a passage of the Royal Research Ship (RRS) "Charles Darwin" on a route from Durban (South Africa) to the Seychelle Islands (Fig. 1). The samples were collected from the ship's non-toxic seawater supply, drawn from a depth of 5 m ten or eleven times a day with hourly samples between 18 h and 24 h local time and every 3-6 h during the rest of the day. The ship's coordinates and seawater temperature were recorded at the time of sampling.

Satellite data. Two sources of satellite data were used in this study. Sea surface temperature (SST) measurements were obtained from the TRMM Microwave Imager (TMI), processed by Remote Sensing Systems. TMI is a microwave instrument, enabling SST measurements through clouds. Ocean colour data were recorded by the Sea-viewing Wide Field of View Sensor (SeaWiFS), a visible light sensor on the SeaStar platform, launched by Orb. Image Ltd. The sea surface was observed at 1 km resolution in 8 frequency bands spanning 410 nm to 860 nm. Chlorophyll (Chl) concentration was determined from the radiances observed at 440, 490, 510 and 555 nm (O'Reilly et al. 1998), with the other channels being used in screening for clouds and correction for scattering from the atmosphere. The data used in this study were the daily Level 3 chlorophyll product provided by NASA Goddard Space Flight Centre at a resolution of 9 km. The flow cytometric measurements were compared with both the individual satellite passes and a weekly composite (the latter improves spatial coverage, see Fig. 1).

Flow cytometry. Replicated subsamples of 1.8 ml were taken from each collected sample, fixed with 1% paraformaldehyde (PFA), incubated at 2°C for 24 h and stored at –20°C before being analysed after their return to the laboratory. Ultraplankton (UP) were analysed by

flow cytometry (FACSort, Becton Dickinson, Oxford, UK), using a 15 mW 488 nm laser. Ultraphytoplankton (UPP) groups, namely eukaryotic algae (EA), *Prochlorococcus* spp. (*Pro*) and *Synechococcus* spp. (*Syn*) were enumerated separately on the basis of the differences in their autofluorescence properties and light scattering (Olson et al. 1993, Zubkov et al. 1998) (Fig. 2). Nonautofluorescent, predominantly heterotrophic bacterioplankton (HB) were enumerated after staining with the DNA dye, SYBR® Green I (Marie et al. 1997). Yellow-green beads, 0.5 μm diameter (Polysciences, USA), were used as an internal standard of 90° light side scatter, as well as of red fluorescence. The ratio of the mean side scatter or red fluorescence intensity of a UP group to the respective bead intensity was used to normalise samples and to calculate relative values of side scatter, as an index for mean cellular biomass (Bernard et al. 2000), and red fluorescence as a substitute for mean cellular chlorophyll content (Li 1995).

The absolute concentration of beads in a standard stock suspension was determined by flow cytometric counting of beads in volumes dispensed with an automatic micro-injector (KD Scientific, USA). The ratio of bead abundance to that of UP groups was used to compute the absolute concentration of the latter. The concentration of HB was calculated by subtracting the *Syn* and *Pro* concentrations, determined in unstained samples from the total bacterial concentration. An estimate of total UPP Chl or biomass was a sum of the estimated group specific values. The latter were computed by multiplying the mean relative Chl or side scatter values on group abundance.

Because of their high degree of synchronised division, cell cycle analysis of cyanobacteria was carried out to estimate their growth rates. The stained cyanobacterial cells were discriminated from other bacteria based on their higher red fluorescence due to the presence of Chl. Larger *Syn* cells scattered more light than smaller *Pro* cells. Cyanobacterial cells with a single copy of DNA (G_1 stage) were distinguished from those in which DNA was

replicating (S stage) or already replicated (G_2 stage), and the proportion of cells at S and G_2 stages was monitored during a diurnal cycle. The minimum growth rates of both *Syn* and *Pro* cyanobacteria were calculated according to Vaulot et al. (1995).

Data analysis. Acquisition and preliminary analysis of flow cytometric data were done using CellQuest software (Becton Dickinson, Oxford, UK). Correlation and regression analyses were used for comparison of the data sets at 99% confidence.

Results

The SeaWiFS data revealed the derived Chl concentrations to vary on quite small spatial scales (Fig. 1). High Chl concentrations, associated with upwelling, were found along many parts of the coast of Madagascar and Mozambique. In this region eddies and currents play an important part in the spatial distribution of the Chl signature (Quartly & Srokosz 2003). To the south of Madagascar lies a region of high Chl waters, which have been upwelled near the coast and then entrained by the East Madagascar Current, which flows westward around the south of the island. At 20°S in the Mozambique Channel there is a 100-km wide band of high Chl waters that have been advected into mid channel from the Mozambican coast. De Ruijter et al (2002) have noted four to five anticyclonic eddies per year heading south along the western edge of the channel, and Quartly and Srokosz (2003) have shown the effect these have on the Chl distribution. At the northern end of the channel there is another sharp transition, presumably related to the westward-flowing North Madagascar Current entraining productive waters from the northern tip of the island.

The TMI data showed surface temperatures of around 25°C, with values higher in the shallower regions of the central Mozambique Channel and the approach to the Seychelles (55°E, 5°S). The ship and satellite records of temperature agreed closely (Fig. 3a), with a significant correlation at $P<0.0001$, $r=0.86$. The ship measurements at a depth of 5 m, were systematically 0.8°C lower than the satellite measurements which correspond to the top millimetre of the sea surface.

Encouraged by the agreement of the temperature data sets we compared SeaWiFS Chl measurements with Chl concentration, abundance and biomass of different UP groups. Although SeaWiFS was overflying the studied area daily at about noon local time, SeaWiFS does not cover the entire globe in one day, so there were only simultaneous satellite observations on three out of the seven days of shipboard observations. To increase number of comparisons with satellite measurements we combined all satellite measurements along the ship track during the seven days of onboard sampling. The mean values of Chl concentration are compared with individual observations on Fig. 3b. The coefficient of variance of mean values was relatively low (less than 30%). To reduce the possibility of artificial relationships caused by averaging satellite data, we correlated the weekly composite as well as individual satellite Chl measurements with flow cytometric measurements of UP groups (Fig. 3; Table).

The direct satellite measurements (Fig. 3b, black hexagons) were compared with matched daytime (from 6–18 h local time) measurements of UP parameters, assuming that the ocean colour did not change during the light period (Table, Direct). In order to minimise the effect of diel variability a subset of UP measurements recorded during the daytime was correlated with composite satellite measurements (Table, Daytime). Finally the whole set of onboard UP measurements was compared with the 7-day satellite composite (Table, All). Irrespective of the analysed dataset the EA and UPP Chl correlated strongly with satellite Chl measurements. A similar relationship was found for the *Syn* Chl, except for the comparison of the direct datasets, most likely because of a small dataset combined with high variability of *Syn* cellular Chl content.

Each of the UPP groups comprised a substantial proportion of total UPP Chl: *Syn* 40±17%, EA 30±9% and *Pro* 30±17%. Therefore, the very weak correlation between the *Pro* Chl and satellite Chl require an explanation. We plotted the satellite Chl versus the EA, EA+*Syn* and EA+*Syn*+*Pro* group sums, using the three datasets (Fig. 4). Unsurprisingly, our confidence in the slopes of the regression lines is dependent on the size of the datasets,

emphasising the necessity of increasing the number of observations for more reliable regression approximations. A similar feature of all three plots was the parallel regression lines of the EA+*Syn* and EA+*Syn*+*Pro* group Chl sums that showed that the contribution of *Pro* Chl was similar at all stations despite of the fact that *Pro* Chl concentration varied six fold along the transect. Most likely the SeaWiFS sensor could not detect *Pro* Chl due the physical properties of the *Prochlorococcus* cells, e.g. small cell size – 0.5-0.6 μm, which is comparable to wavelengths of visible light.

One of the sources of variability of the UPP group Chl is diel change in cellular Chl content (Jacquet et al. 2002). We reduced the diel effect by using only daytime cellular Chl data. For each individual day we compared mean Chl contents of the UPP groups using only measurements taken at 9, 12 and 15 h local time (as the relevant satellite overpass is near noon local time), and multiplied these mean values by the concentration of cell determined during the particular day, 'averaged daytime' chlorophyll. The diel correction increased the correlations for the EA, *Syn* and UPP Chl (Table), confirming that diel cellular Chl variation made a moderate contribution towards spatio-temporal variability of the group Chl fields. However, although *Prochlorococcus* had the most significant diel variation the correction had no effect on its relationship with satellite Chl, supporting our speculation that the satellite instrument could not detect *Pro* Chl.

If one decides to employ real time satellite colour data to parameterise marine ecosystem models, the strong empirical relationships between the satellite Chl and the EA and *Syn* Chl measurements would have limited usefulness, because addition conversion factors are required for converting the UPP group Chl estimates into the group abundance or biomass. To reduce a number of conversion steps we looked for direct correlation between the latter two parameters and the satellite Chl (Table). Among the ultraplankton only EA and HB group abundances have similarly strong relationship with the satellite Chl. Compared to the low variability of the EA and *Pro* cellular Chl contents (3 times and 4.3 times, respectively) *Syn*

cellular Chl varied 12 times and, consequently, the correlation between *Syn* abundance and satellite Chl was weaker than the correlation between *Syn* Chl and satellite Chl measurements. As *Pro* has its greatest abundance in oligotrophic (Chl poor) waters, it has a weak negative correlation with the satellite Chl measurements.

The satellite data would be even more useful for modelling if one can use them for approximation of the UP group biomass. In the present study side scatter of the UP groups was used as an index of cellular biomass. Only *Pro* cellular side scatter correlated strongly with the *Pro* cellular Chl content ($r=0.8$, $P<0.0001$). However, because no significant relationship was found between satellite Chl measurements and *Pro* Chl concentration, there were also very weak correlation between *Pro* biomass and satellite Chl. Similarly to the abundance data only the EA and HB group biomasses showed strong correlation with the satellite data.

Discussion

The strong relationships found between the SeaWiFS Chl concentrations and abundance and biomass of EA and HB (Figs. 3b,c & 4) are very encouraging, because there is a potential for estimating concentrations of these two groups from satellite Chl data using linear regressions. For example: EA [cells ml^{-1}] = -670±200 + 12000±850 × Chl [ng ml^{-1}]; HB [cells ml^{-1}] = 320000±32000 + 1900000±140000 × Chl [ng ml^{-1}]. The negative intercept of the EA regression can be explained by the fact that eukaryotic algae represent only part of a phytoplankton community, the total chlorophyll amount of which is determined by the satellite.

On the other hand the satellite data used in this comparison contained no values below 0.1 mg m^{-3}, whereas the cytomatric measurements at a number of stations showed minimal concentrations of EA, *Syn* and *Pro* (see Fig. 4). In general the SeaWiFS algorithm can yield chlorophyll concentrations below 0.05 mg m^{-3}, so there would appear to be a bias in the particular satellite dataset used here. This could be due to the satellite detecting chlorophyll much deeper in the water column than the 5 m depth intake for the underway water supply

system, or it could be due to thin undetected cloud increasing the atmospheric radiance, leading to a local bias in satellite-derived chlorophyll values.

Higher concentration of total Chl would mean higher concentration of phytoplankton in general and EA in particular; and higher phytoplankton concentration leads to more organic nutrients for sustaining higher HB concentration. Using EA and HB groups (Fig. 3c) as indicators of productivity, one can speculate that the northern part of the Mozambique Channel, characterised by warmer waters (Fig. 3a), was probably of lower productivity than the other traversed regions. The sharp decrease of temperature in the proximity of the northern tip of Madagascar indicated the water mass change and coincided with the increase in the EA, HB group as well as total Chl concentrations.

Strong correlation between total chlorophyll measurements and HB abundance is well documented for various aquatic systems (e.g. Simon et al. 1992). An explanation of this relationship requires an assumption of steady state of the microbial planktonic community. Heterotrophic bacteria populating the open oceanic waters are dependent on phytoplankton as the ultimate source of organic nutrients, and in the studied area the microbial community was in homeostasis. There has been considerable doubt that concentrations of unpigmented heterotrophic bacteria are likely to be approximated by remotely sensed parameters, e.g. (Zubkov et al. 2002), and before generalising we would like to check the robustness of observed relationships in other oceanic regions and during other seasons.

The abundances of *Pro* and *Syn* cyanobacteria showed a weak correlation with satellite measurements (Table). In case of *Syn* it was most likely due to high variability of cellular Chl content. In case of *Pro* the relationship with Chl was negative, because usually the abundance of these cyanobacteria is greater in more oligotrophic and consequently Chl depleted waters (Partensky et al. 1999). Our attempts to use other SeaWiFS wave band measurements (e.g. 555±10 nm) for correlating with *Syn* concentrations, exploiting their unique phycoerythrin orange fluorescence, were not successful.

For the required spatial coverage the satellite images collected over a period of several days had to be composited, and consequently the temporal resolution was sacrificed. Both EA and HB, comprised of many different species, and consequently did not show pronounced diel cycles. Highly variable *Syn* and *Pro* abundance (Fig. 3d) were clearly controlled at hourly scale not by nutrient sources, i.e. a "bottom up" factor (Verity & Smetacek 1996), but more likely by a dynamic equilibrium of synchronised replication (Vaulot et al. 1995), and mortality – predatory pressure and/or viral infection, i.e. a "top down" factor. The primary cause of the high variability of cyanobacterial abundance was a remarkable diel synchronisation of both *Syn* and *Pro* cell division along the track (Fig. 3e) with estimated minimum growth rates of 0.25±0.037 and 0.35±0.042 d^{-1} averaged for six full diel cycles, respectively. Up to 60% of *Syn* and *Pro* cells were generally going into division after dusk between 18-22 h. Similar division patterns of cyanobacteria were observed both in the Pacific (Vaulot et al. 1995) and Atlantic (Partensky et al. 1999, Zubkov et al. 2000a) Oceans, showing that this phenomenon appears to be global. The average minimum growth rate of *Pro* in the Mozambique Channel was about one third of *Pro* growth in the Equatorial Pacific and twice as high as estimated *Pro* growth in the oligotrophic Atlantic Ocean. The high diel variability seemed the most plausible explanation of the weak relationship between cyanobacterial abundance/biomass and satellite data; however, we were able to determine that it was not the main cause.

Thus, the present study demonstrates the utility of a combination of flow cytometry and satellite remote sensing in surveying ultraplankton. It shows both the great potential and also certain limitations of current satellite remote sensing methodology. There is a possibility of using parameters like ocean colour for predicting distribution of ultraplanktonic organisms like eukaryotic algae and even heterotrophic bacteria. New spaceborne sensors with improved spatial and spectral resolution, such as MERIS on Envisat (Rast et al. 1999), may better enable the quantification of separate pigment concentrations, and thus classification of the different phytoplanktonic groups present. However, monitoring of cyanobacteria from space will

probably remain a challenge, until satellite instrument sensitivity is significantly improved and model corrections for diel cellular pigment adaptations are established and parameterised.

Acknowledgements

We thank officers and crew aboard the RRS Charles Darwin for assistance and the two anonymous reviewers for helpful comments on the earlier version of this paper. The authors would like to thank the SeaWiFS Project (Code 970.2) and the Distributed Active Archive Center (Code 902) at the Goddard Space Flight Center, Greenbelt, MD 20771, for the production and distribution of these data, respectively. These activities are sponsored by NASA's Mission to Planet Earth Program. TMI data and images are produced by Remote Sensing Systems and sponsored by NASA's Earth Science Information Partnerships (ESIP) and by NASA's TRMM Science Team. This work forms part of the Natural Environment Research Council (NERC) Marine and Freshwater microbial biodiversity programme (NER/T/S/2000/00635). The research of M.V.Z. was supported by the advanced research fellowship (NER/I/S/2000/00898) from NERC.

References

Behrenfeld MJ, Falkowski PG (1997) Photosynthetic rates derived from satellite-based chlorophyll concentration. Limnol Oceanogr 42:1-20

Bernard L, Courties C, Servais P, Troussellier M, Petit M, Lebaron P (2000) Relationships among bacterial cell size, productivity, and genetic diversity in aquatic environments using cell sorting and flow cytometry. Microb Ecol 40:148-158

Buck KR, Chavez FP, Campbell L (1996) Basin-wide distributions of living carbon components and the inverted trophic pyramid of the central gyre of the North Atlantic Ocean, summer 1993. Aquat Microb Ecol 10:283-298

Chisholm SW, Olson RJ, Zettler ER, Goericke R, Waterbury JB, Welschmeyer NA (1988) A novel free-living prochlorophyte abundant in the oceanic euphotic zone. Nature 334:340-343

de Ruijter WPM, Ridderinkhof H, Lutjeharms JRE, Schouten MW, Veth C (2002) Observations of the flow in the Mozambique Channel. Geophys Res Lett 29: 140:1-4. DOI 10.1029/2001GL013714.

Garcon VC, Oschlies A, Doney SC, McGillicuddy D, Waniek J (2001) The role of mesoscale variability on plankton dynamics in the North Atlantic. Deep Sea Res II 48:2199-2226

Jacquet S, Prieur L, Avois-Jacquet C, Lennon JF, Vaulot D (2002) Short-timescale variability of picophytoplankton abundance and cellular parameters in surface waters of the Alboran Sea (western Mediterranean). J Plankton Res 24:635-651

Li WKW (1995) Composition of ultraphytoplankton in the central North Atlantic. Mar Ecol Prog Ser 122:1-8

Li WKW, Harrison WG (2001) Chlorophyll, bacteria and picophytoplankton in ecological provinces of the North Atlantic. Deep Sea Res II 48:2271-2293

Maranon E, Holligan PM, Barciela R, Gonzalez N, Mourino B, Pazo MJ, Varela M (2001) Patterns of phytoplankton size structure and productivity in contrasting open-ocean environments. Mar Ecol Prog Ser 216:43-56

Marie D, Partensky F, Jacquet S, Vaulot D (1997) Enumeration and cell cycle analysis of natural populations of marine picoplankton by flow cytometry using the nucleic acid stain SYBR Green I. Appl Environ Microbiol 63:186-193

Morel A, Ahn Y-H, Partensky F, Vaulot D, Claustre H (1993) *Prochlorococcus* and *Synechococcus*: A comparative study of their optical properties in relation to their size and pigmentation. J Mar Res 51:617-649

Olson RJ, Zettler ER, DuRand MD (1993) Phytoplankton analysis using flow cytometry. In: Kemp PF, Sherr BF, Sherr EB, Cole JJ (eds) Handbook of methods in aquatic microbial ecology. Lewis Publishers, Boca Raton, Florida, p 175-186

O'Reilly JE, Maritorena S, Mitchell BG, Siegel DA, Carder KL, Garver SA, Kahru M, McClain C (1998) Ocean color chlorophyll algorithms for SeaWiFS. J Geophys Res-Oceans 103:24937-24953

Partensky F, Hess WR, Vaulot D (1999) *Prochlorococcus*, a marine photosynthetic prokaryote of global significance. Microbiol Mol Biol Rev 63:106-127

Quartly GD, Srokosz MA (2003) Eddies in the southern Mozambique Channel, Deep Sea Res II, accepted

Rast M, Bezy JL, Bruzzi S (1999) The ESA Medium Resolution Imaging Spectrometer MERIS - a review of the instrument and its mission. Int J Remote Sens 20:1681-1702

Simon M, Cho BC, Azam F (1992) Significance of bacterial biomass in lakes and the ocean - comparison to phytoplankton biomass and biogeochemical implications. Mar Ecol Prog Ser 86:103-110

Vaulot D, Marie D, Olson RJ, Chisholm SW (1995) Growth of *Prochlorococcus*, a photosynthetic prokaryote, in the equatorial Pacific ocean. Science 268:1480-1482

Verity PG, Smetacek V (1996) Organism life cycles, predation, and the structure of marine pelagic ecosystems. Mar Ecol Prog Ser 130:277-293

Waterbury JB, Watson SW, Guillard RRL, Brand LE (1979) Wide-spread occurence of a unicellular, marine planktonic, cyanobacterium. Nature 277:293-294

Zubkov MV, Fuchs BM, Tarran GA, Burkill PH, Amann R (2002) Mesoscale distribution of dominant bacterioplankton groups in the northern North Sea in early summer. Aquat Microb Ecol 29:135-144

Zubkov MV, Sleigh MA, Burkill PH (2000a) Assaying picoplankton distribution by flow cytometry of underway samples collected along a meridional transect across the Atlantic Ocean. Aquat Microb Ecol 21:13-20

Zubkov MV, Sleigh MA, Burkill PH, Leakey RJG (2000b) Picoplankton community structure on the Atlantic Meridional Transect: a comparison between seasons. Prog Oceanog 45:369-386

Zubkov MV, Sleigh MA, Tarran GA, Burkill PH, Leakey RJG (1998) Picoplanktonic community structure on an Atlantic transect from 50 degrees N to 50 degrees S. Deep Sea Res I 45:1339-1355

Table. Pearson correlation coefficients and their significance (given by asterisks) for the various observed relationships between the SeaWiFS chlorophyll concentrations and flow cytometric estimates of ultraplankton group measurements, such as chlorophyll concentrations, abundance and biomass, done between dawn and dusk on the day of satellite measurement (Direct), during the daylight period (Daytime), as well as with a complete dataset of the transect measurements (All).

Variables	SeaWiFS Chlorophyll		
	Direct [n=12]	Daytime [n=30]	All [n=63]
Chlorophyll			
Eukaryotic algae	**0.97*****	**0.83*****	**0.86*****
Prochlorococcus	0.27	0.03	0.32*
Synechococcus	0.57	**0.88*****	**0.85*****
Total ultraphytoplankton	**0.81***	**0.93*****	**0.89*****
Averaged Daytime Chlorophyll			
Eukaryotic algae	**0.94*****	**0.84*****	**0.89*****
Prochlorococcus	0.05	-0.03	0.02
Synechococcus	**0.85****	**0.84*****	**0.83*****
Total ultraphytoplankton	**0.92*****	**0.89*****	**0.88*****
Abundance			
Eukaryotic algae	**0.93*****	**0.84*****	**0.87*****
Prochlorococcus	-0.7*	-0.56*	-0.48**
Synechococcus	-0.01	0.67*	0.59***
Heterotrophic bacteria	**0.91*****	**0.89*****	**0.87*****
Biomass			
Eukaryotic algae	**0.8***	0.79**	**0.82*****
Prochlorococcus	-0.57	-0.45	-0.38*
Synechococcus	0.11	0.67*	0.57***
Total ultraphytoplankton	-0.01	0.45	0.44**
Heterotrophic bacteria	**0.92*****	**0.86*****	**0.86*****

To assist reading the table Pearson coefficients of correlation higher than 0.8 are marked in bold. Probability symbols at 99% confidence are: difference between two values insignificant - P>0.01; significant - * P<0.01, ** P<0.001, *** P<0.0001

Figure legends

Fig. 1. A composite satellite image (SeaWiFS) of chlorophyll spatial distribution in the Mozambique Channel on 23-29 August 2001, with the track of RRS "Charles Darwin" superposed.

Fig. 2. Characteristic flow cytometric signatures of natural ultraphytoplankton in the Mozambique Channel (a, b) and at the approaches to the Seychelles (c, d). The *Synechococcus* (*Syn*, a, c) cluster was revealed by its specific orange phycoerythrin (phyc) autofluorescence and excluded from the chlorophyll (chl) plots (b, d). The *Prochlorococcus* (*Pro*, b, d) and eukaryotic algae (EA, b, d) clusters were clearly resolved by their red chlorophyll autofluorescence. Yellow-green beads, 0.5 μm diameter, were used as an internal standard.

Fig. 3. Latitudinal distribution of the shipboard (black diamonds) and satellite (grey diamonds) sea surface temperature (a); composite mean (grey hexagons) and direct (black hexagons) concentrations of chlorophyll (Chl) measured by SeaWiFS satellite, error bars show single standard deviations (b); heterotrophic bacteria (HB) and eukaryotic algae (EA) (c); *Synechococcus* and *Prochlorococcus* abundance in surface waters (*Syn* & *Pro*) (d) and temporal variation of percentages of dividing cyanobacterial cells (e) along the ship track (see d for symbol legend). Thick lines at the bottom show night periods.

Fig. 4. Comparison of SeaWiFS chlorophyll measurements with matched/direct (a), daytime (b) and all (c) measurements of chlorophyll concentrations of ultraphytoplankton (UPP) groups: eukaryotic algae (EA) plus *Synechococcus* (*Syn*) and plus *Prochlorococcus* (*Pro*) in relative units (r.u.). Lines indicate linear regressions. Corresponding slope values are shown outside the plots. See details in the text and Table.

Fig. 1

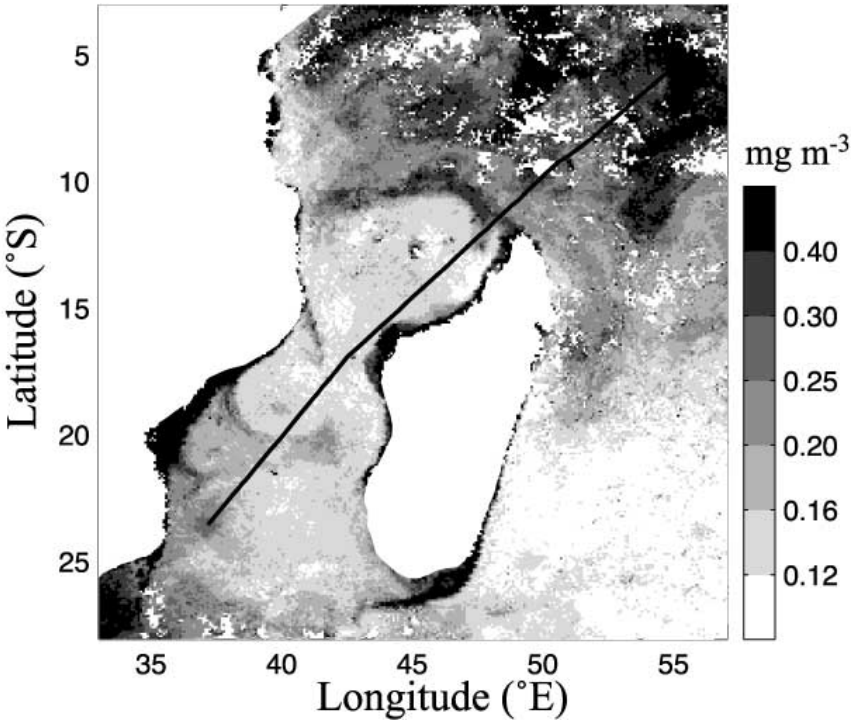
5
10
15
20
25
Latitude (°S)
35
40
45
50
55
Longitude (°E)
mg m-3
0.40
0.30
0.25
0.20
0.16
0.12

1 Fig . 2

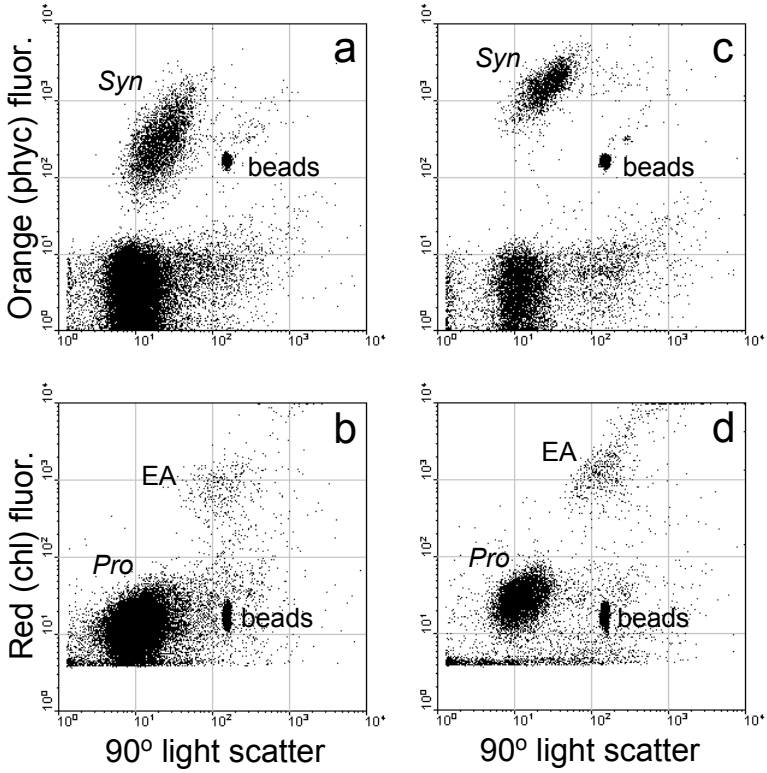
a
b
c
d
Syn
beads
EA
Pro
Orange (phyc) fluor.
Red (chl) fluor.
90º light scatter
90º light scatter

2
3

Fig. 3

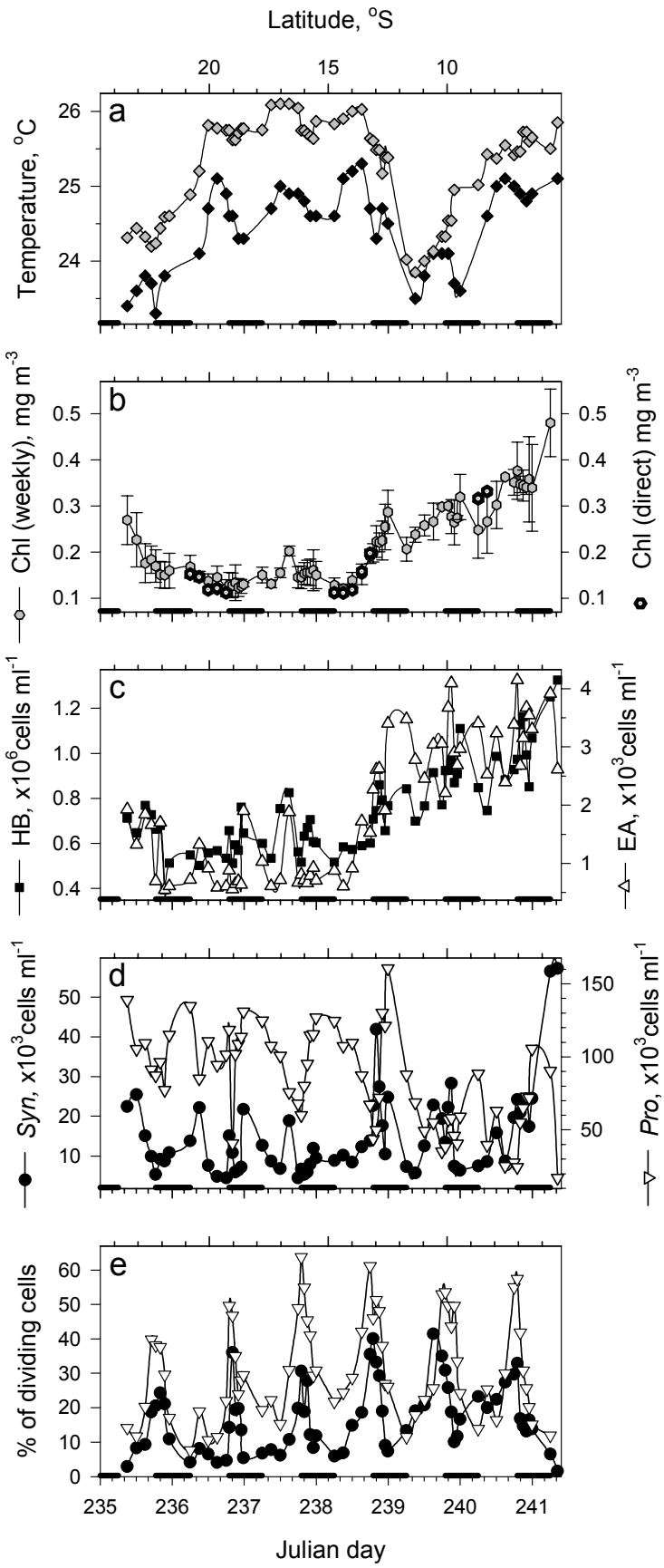
Latitude, °S
20
15
10
a
Temperature, °C
26
25
24
b
Chl (weekly), mg m-3
Chl (direct) mg m-3
0.5
0.4
0.3
0.2
0.1
c
HB, x10^6cells ml-1
EA, x10^3cells ml-1
1.2
1.0
0.8
0.6
0.4
4
3
2
1
d
Syn, x10^3cells ml-1
Pro, x10^3cells ml-1
50
40
30
20
10
150
100
50
e
% of dividing cells
60
50
40
30
20
10
0
235
236
237
238
239
240
241
Julian day

1 Fig. 4

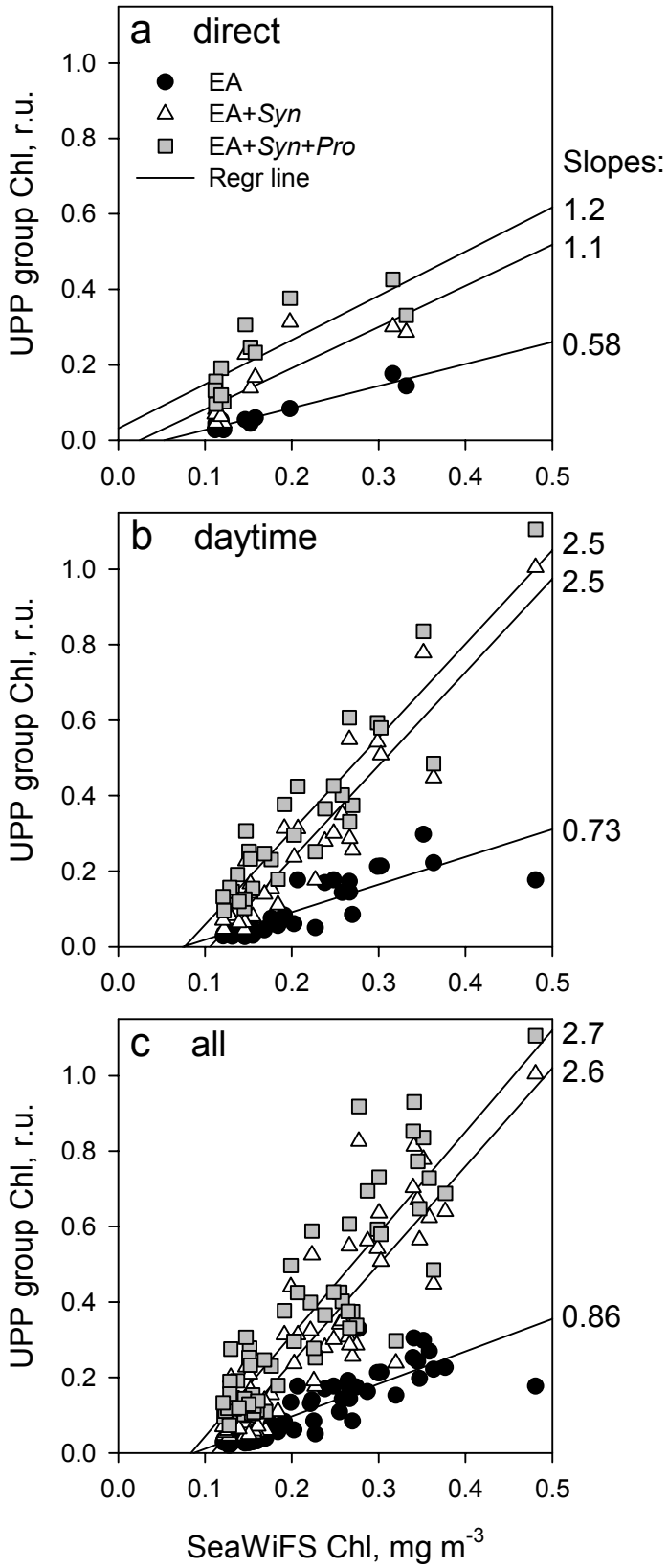
a direct
EA
EA+Syn
EA+Syn+Pro
Regr line
Slopes:
1.2
1.1
0.58
b daytime
2.5
2.5
0.73
c all
2.7
2.6
0.86
UPP group Chl, r.u.
SeaWiFS Chl, mg m-3
0.0
0.2
0.4
0.6
0.8
1.0
0.1
0.3
0.5

2